1-2 Mesosphere Observations: Dynamics and Chemistry / Material in the Upper Air

Characteristics of Aerosol in the Polar Mesosphere Derived from Rayleigh Lidar Observations

SAKANOI Kazuyo, MURAYAMA Yasuhiro, Richard L. COLLINS, and MIZUTANI Kouhei

In this paper, we present characteristics of aerosol in the polar mesosphere derived from Rayleigh lidar observations over Poker Flat Research Range, Univ. of Alaska, Fairbanks. There are two kinds of aerosol, noctilucent clouds and rocket plume. At first, we show that aerosol of noctilucent clouds are transported by background wind. Then extent of the rocket plume can be estimated from lidar data considering their transport by background wind. This kind of measurements is useful to new research in the mesosphere.

1 Introduction

Numerous techniques are available for observing the terrestrial atmosphere. It is relatively easy to take in situ measurements of meteorological parameters near the surface — an area with which we are well familiar — such as temperature, humidity, aerosols (minute particles suspended in air, such as dust), and wind velocity. However, as the terrestrial atmosphere stretches upward to an altitude of $300-400$ km, these meteorological observations become more difficult with increasing distance from the ground.

From 1997 to 1998, NICT installed and began operation of a Rayleigh lidar and an MF radar at the Poker Flat Research Range (PFRR: N 65.1°, W 147.5°), University of Alaska, Fairbanks, located in Chatanika in the suburbs of Fairbanks, as part of joint US-Japan research with the University commonly known as the "Alaska Project". These instruments are remote-sensing devices for the terrestrial middle atmosphere. The Rayleigh lidar can measure atmospheric density, temperature, and aerosols at altitudes of approx. $40-90$ km, and the MF radar measures wind velocity and electron density at $60-100$ km. The range of altitudes measured by these two instruments (approx. $40-90$ km) corresponds to the upper stratosphere and mesosphere of the terrestrial atmosphere, and is higher than the altitudes at which flying objects such as aircraft and sondes operate, and lower than the operational altitudes of rockets, space shuttles, and satellites. In this region, in situ measurements are
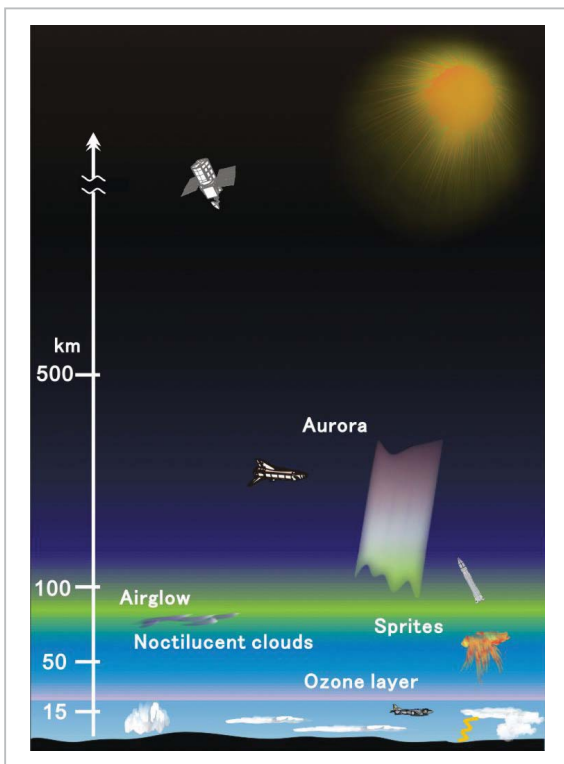
Fig.1 *Various meteorological phenomena in the terrestrial atmosphere and flying objects used in observations*

Fig.2 *Noctilucent clouds observed over the Poker Flat Research Range*

not possible, leaving remote-sensing techniques as the only meteorological observation methods available.

In the past, it was believed that aerosols and water vapor did not exist in the upper stratosphere and mesosphere, due to the great distances from the ground; it was further believed that atmospheric activities such as convection did not take place on a significant scale. However, in the 1880s, bright white clouds designated "noctilucent clouds" were first observed at dusk over the polar regions. As studies on the characteristics of the clouds progressed, it became clear that noctilucent clouds occurred at high altitudes of approx. 80 km, heights previously unheard of for clouds (normal clouds form at altitudes below 15 km)[1]. Furthermore, these clouds often displayed characteristic wavelike structures, evidence that high atmospheric activity did indeed exist at these altitudes.

It was further revealed that the cloud was an ice-particle cloud having some dust species as its nucleus. This indicated the possibility of

the presence of water vapor at these altitudes, despite previous predictions to the contrary. It must be noted that an increase in methane gas, a green house gas, leads to an increase in water vapor in the mesosphere. Moreover, an increase in carbon dioxide lowers the temperature of the mesosphere through the intensification of infrared radiation cooling. These two conditions favor the generation of noctilucent clouds, and some research groups have proposed that such clouds may be used as indicators of global environmental change[2].

The Rayleigh lidar emits a high-power laser pulse vertically into the atmosphere, and atmospheric measurements are made by collecting the scattered light of this transmitted laser pulse using a receiving system (telescope). In the absence of notable volumes of aerosols in the atmosphere, the lidar receives the laser beam scattered by atmospheric molecules (Rayleigh scattering); in this case the intensity of the received signal should simply be proportional to atmospheric density. In contrast, with significant volumes of aerosols present in the atmosphere, the intensity of the Mie-scattered light due to these aerosols will increase, and the received signal will display intensity variations that are dependent on the density and particle-size distribution of the aerosols, instead of on atmospheric density.

In this paper, we will provide a brief explanation on the characteristics of polar mesospheric aerosols (i.e., noctilucent clouds) obtained from measurements using the

Rayleigh lidar. We will then present the initial results of measurements taken of rocket plumes (artificial mesospheric aerosols) with the Rayleigh lidar during one of the occasional rocket launches at PFRR. We will point out some of the potential of artificial aerosol observations in the mesosphere as a technique for detailed middle atmosphere observation.

2 Measurement instrument and analysis data

2.1 The Rayleigh lidar

The Rayleigh lidar was installed at PFRR in Nov. 1997, and it is still in operation today[3]. The transmission system uses an Nd:YAG laser. The wavelength is 532-nm, the secondary harmonic wave of the laser. The transmission pulse has a repetition frequency of 20 Hz, pulse energy of 550 mJ, and beam spread of < 0.1 mrad. The receiving system uses a Newtonian telescope having a diameter of 61 cm, F3.1, and a field of view of 1.6 mrad.

The altitude range of measurements is 35 – 80 km, and the vertical profile of atmospheric density and temperature can be measured at temporal resolution of 2.5 min. and height resolution of 75 m. Above 35 km, aerosols are absent in the atmosphere, and so the received signal is composed solely of Rayleigh-scattered light from atmospheric molecules. Therefore, the signal intensity is proportional to atmospheric density, and decreases with increasing altitude. After the atmospheric density has been calculated from the received signal, atmospheric temperature is determined using the hydrostatic equation. With this method, we are able to calculate atmospheric temperature with a precision of ±5 K below an altitude of 70 km.

In this work, we used Mie-scattered light from irregular occurrences of mesospheric aerosols, such as noctilucent clouds and rocket plumes. In this case, the received signal intensities should display intensity variations that are dependent on both density and particle sizes of the scattering materials. Thus, unless the latter is known, the former cannot be cal-

culated. Since it is impossible to determine the particle-size distribution based on Rayleigh lidar data, we will hereafter focus our discussions simply on the vertical profiles and temporal variations of the received signal intensity.

2.2 The MF radar

The MF radar was installed in Oct. 1998, and remains in operation.[4]. The altitudinal range of the observation is 60 – 100 km, and the electron density in the atmosphere and wind velocities are derived using the signals partially reflected by ionized gas (ionosphere) and those scattered due to disturbances at these altitudes. The radar transmits a 2.43-MHz radio signal in the vertical direction at a peak power of 50 kW. The height and temporal resolutions are of 4 km and 3 min., respectively. Observations can be made both during the daytime and nighttime. Wind velocity is determined by the correlation method, and electron density is estimated using the polarization of the radio wave. In this work, wind velocity data averaged over 30 minutes or 4 hours is used as the background wind velocity field data to examine aerosol motion.

2.3 Digital single-lens reflex camera for automatic observation

In order to monitor the shape, spread, and motion of the noctilucent clouds, we installed a digital single-lens reflex camera for automatic observation in March 2004, which remains in operation today[5]. The instrument is a combination of a commercially-available single-lens reflex camera and a fish-eye lens and automatically captures digital images. Dedicated software controls the device, and allows variable remote-settings of pixels, photo interval, sensitivity, exposure, and aperture. During noctilucent cloud observations, images are taken in one-minute or four-minute intervals and are stored at three different resolutions. The field of view is pointed northward from the PFRR, and the noctilucent cloud appears in the region from the northern horizon (on a fringe of an image) to the center of

the image. Sensitivity is set in the automatic mode.

Although the camera does not perform precise calibrations for field of view or sensitivity, it is possible to estimate the angle of view from the stars that are included in the image. The values for the shape and motion of the noctilucent clouds calculated in this paper are based on the altitude and orientation estimated with these stars as the reference.

3 Observation of noctilucent clouds

3.1 The mesosphere and noctilucent clouds

The terrestrial atmosphere is divided into four regions, depending on whether temperature increases or decreases with increasing altitude. The region from the ground surface to an altitude of approx. 15 km is called the troposphere (temperature decreases with altitude), 15–55 km is the stratosphere (temperature increases with altitude), 55–90 km is the mesosphere (temperature decreases with altitude), and 90 km to the thermopause (300–400 km) is the thermosphere (temperature increases with altitude). The boundary between the mesosphere and the thermosphere is called the mesopause, and in the summer polar regions, the mesopause is located near an altitude of 87 km. Also in the summer polar region, the mesopause is the coldest region in the terrestrial atmosphere, with temperatures that may fall below 130–150 K[6]. Generally, temperature decreases with increasing latitude at the identical altitude.

The noctilucent cloud is an ice-particle cloud that forms under these extreme low-temperature conditions. Ice-forming nuclei are necessary for the formation of noctilucent clouds, and it is considered that the materials that constitute the nuclei of these clouds are metal atoms of comet origin or proton hydrates (supersaturated hydrogen ions). A nuclear diameter of at least 20 nm is required for a noctilucent cloud to be observed by the Rayleigh lidar, and so lidar observation will cover the relatively large particle-size range of the cloud particle size distribution.

The formation and dissipation processes of the noctilucent cloud are considered to be as follows. First, ice begins forming around the nuclei near the 87-km altitude region where the temperature is at the minimum. Then, as the ice particles grow in size, the cloud particles become heavier and begin to fall due to gravity. However, there exists the upward flow in the summer polar mesosphere, the falling velocity is determined by the balance with the upward flow. The ice particle continues to attract water vapor and grow during its fall, and eventually it acquires a diameter large enough to be detected by the Rayleigh lidar. At this point, the altitude is approximately 84–80 km. Since the temperature increases with decreasing altitude in the mesosphere, the ice particles melt and evaporate after they reach a certain altitude (corresponding to the lowest altitude of lidar signals), and return to vapor form. This cycle is repeated[7].

3.2 Results of noctilucent cloud observation

Figures 3 and 4 show the signals scattered from the noctilucent cloud detected by the Rayleigh lidar on the nights of August 4–5, 1999 and August 3–4, 2002. In the figures, the vertical profiles of the lidar signal intensities are aligned in a time series every two and a half minutes. The horizontal axis represents the relative intensities of the received signals, and for each profile, the axis is shifted by 100. The vertical axis represents altitude. Time is represented in local standard time [AKST] without daylight saving time. Since observations were performed continuously from the previous night, 12 o'clock midnight is described as 24:00, and 1 o'clock in the morning as 25:00. Note that the solar elevation is lowest near 25:00 [AKST].

During both periods, only the Rayleigh-scattered light from the atmosphere is observed in the initial stages of observation. Then, from about 24:45 [AKST], Mie-scattered signals from a noctilucent cloud near the
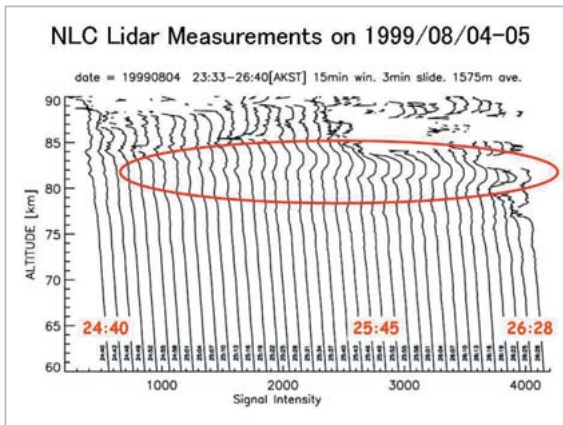
Fig.3 *Time series of the vertical profiles of lidar observation data for August 4-5, 1999*
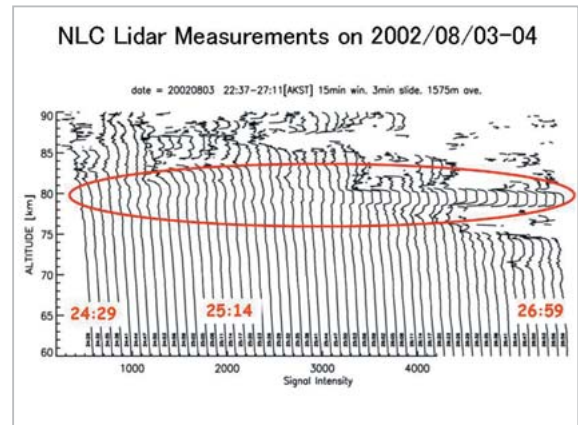
Fig.4 *Time series of the vertical profiles of lidar observation data for August 3-4, 2002*

83-km and 80-km altitudes begin to appear. The intensities of these signals increase with time, and reach their near-maximum values at the termination of observation (26:00-27:00 [AKST]). Note that the lidar observations can only be made during the hours of darkness, and so the noctilucent clouds may have been present for some time after the observations.

A summary of representative noctilucent clouds during the period from 1999 to 2005 is shown in Table 1. The time during which signals were received from the noctilucent cloud is shown in the "Time" column, and in the case when received signals were interrupted by the beginning or termination of observation, this value appears in brackets. Figure 5 shows four images of noctilucent clouds on the night of August 5-6, 2004. In each image, the lower and upper sides correspond to north and south, respectively, and the left and right sides correspond to west and east, respectively. The images show the evolution of the noctilucent cloud from 25:25 in 10-minute intervals, in sequential order as follows: top left, bottom left, top right, bottom right. The circles at the center of the image indicate where a fixed portion of the cloud was located at the corresponding observation time. The solid black line shows the horizontal position of the circle at the beginning of the series.

The circles in the images move toward the top of the panel, that is from north to south. Similar motion of the noctilucent cloud is often observed in other nights. The motion along the N-S axis is always directed southward. The motion along the E-W axis is generally directed westward, although motion in the reverse directions are observed in some instances. Estimation of noctilucent cloud speed, which is derived from estimated altitudes and orientations of the cloud using stars as positional references, is in the range of approx. 20-70 m/sec in both the N-S and E-W directions.

3.3 Occurrence and motion of the noctilucent clouds and mesospheric winds

Table 1 shows the initial detection of lidar signals from noctilucent clouds around 24:00, with detection continuing until the end of observation. On the other hand, the clouds become apparent in digital camera images from around 23:00. It is considered that the time lag between lidar and digital-camera detection is due to the wider field of view of the digital camera, which permits observation from the northern horizon to directly above the observation point. The lidar features a narrower view, and can only detect signals directly above the observation point.

Based on the characteristics of the occurrence period and motion shown in Fig. 5, it is suggested that the noctilucent clouds are transported by winds from the regions nearer to the pole (northwards) where the formation and

dissipation of the noctilucent clouds occur. In order to confirm this model, we investigated wind velocity measured using the MF radar. Figures 6 and 7 present mesospheric wind velocities on August 8–11, 2005 in color contours, as an example. The vertical and horizontal axes represent the altitude and the date/time (in Universal Time), respectively. The time zone enclosed in the red square represents the time of occurrence of the noctilucent cloud.

In Fig. 6, both northward (green) and southward (blue) winds can be seen, but in general, the blue and green regions appear

Table 1 *Summary of the Representative Noctilucent Cloud Data from Summer 1999 to Summer 2005*

Date	Time[AKST]	Height	Extent	Instrument
99/08/05	24:45 – (26:28)	81 - 83km	?	Lidar
02/08/01	24:52 – (25:52)	77 – 78 km	?	Lidar
02/08/04	24:44 – (26:59)	79 - 81km	?	Lidar
03/08/07	25:25 – (26:58)	80 – 83 km	?	Lidar
04/08/03	24:35 – (26:03)	?	Elevation <10°	Camera
04/08/05	(23:00 – 25:45)	?	Elevation ~30°	Camera
04/08/06	(23:21 – 26:15)	?	Elevation ~ 50°	Camera
04/08/09	(23:00) – 26:43	?	Elevation ~25°	Camera
05/08/09	(23:30 – 27:30)	81 – 84 km	Elevation ~ 30°	Lidar Camera
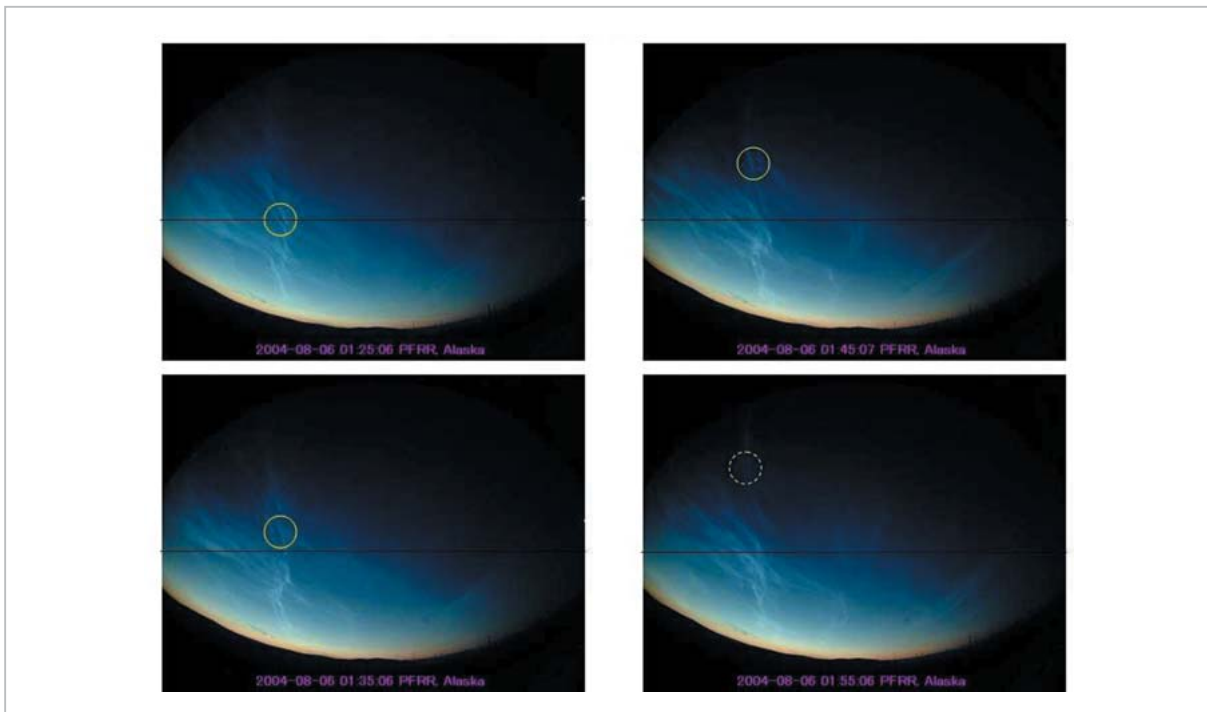
Fig.5 *Images of a noctilucent cloud observed on August 5–6, 2004.*

almost periodically twice per day, as indicated by the two yellow lines. At altitudes of 70‒90 km during the time period in which noctilucent clouds appear, the winds are southward at speeds of 0‒70 m/sec. In Figure 7, a strong westward wind of approx. 50 m/sec prevails constantly, but at altitudes of 83‒90 km, the wind occasionally shifted eastward. These trends are seen every summer.

The direction/velocity of winds and noctilucent cloud motion are consistent, strongly implying that the noctilucent clouds are transported by these winds. Furthermore, there seems to be a periodic increasing and decreasing (reversal) of the southward wind. The timing of the appearance of the noctilucent cloud occurs approximately 3 hours after the increase in the southward wind, that is 3 hours prior to the time at which the southward wind reaches its maximum. These observations also support the model that the timing of noctilucent cloud appearance and its intensification over time are determined by the transport of

the cloud by winds.

4 Rocket plume observation

4.1 Example of lidar detection of rocket plume

At the PFRR, rockets are occasionally launched for scientific observation. The lidar observation point is located approximately 1 km southeast of the rocket launch site. Rockets are launched toward the north, and so they move away from the lidar site. Figure 8 shows the data for a rocket plume detected by the Rayleigh lidar on the night of January 21‒22, 1999. The panels show data every two and a half minutes, from left to right. The horizontal and vertical axes represent signal intensity and altitude, respectively. The solid line slanting to the left toward the top superposed on the signals represents the calculated signal intensity assuming only atmospheric scattering. The dashed lines on both sides of the solid line are the standard deviations of the calculated sig-
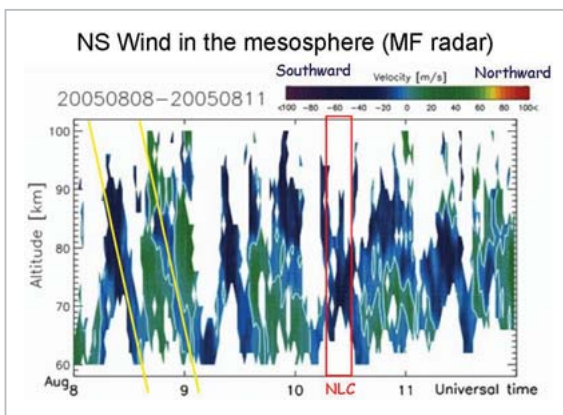
Fig.6   N–S mesospheric wind velocities for August 8–11, 2005
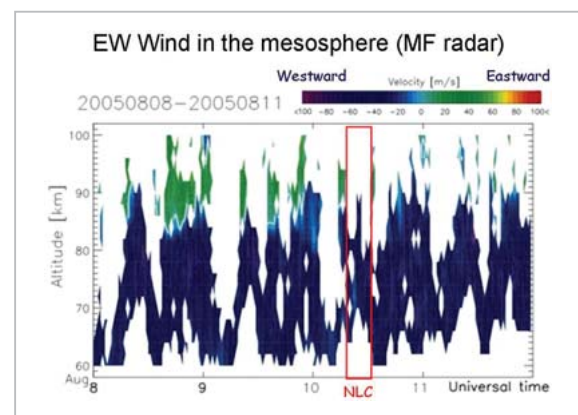
Fig.7   E–W mesospheric wind velocities for August 8–11, 2005
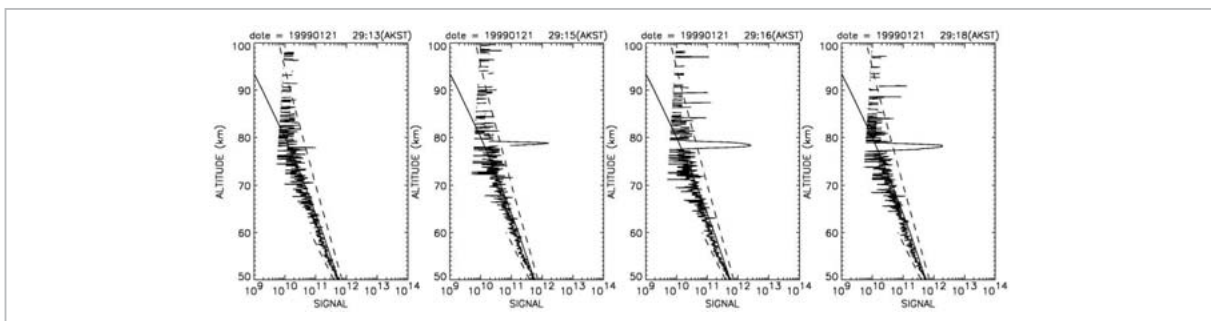
Fig.8   Example of rocket plume observation by the Rayleigh lidar (January 21–22, 1999)

nals.

Near an altitude of 78 km, a layer of strong signals deviate widely from the calculated signal intensity. These signals correspond to the detected rocket plume. Analysis of such lidar signals from three rocket plumes has been performed. Table 2 shows the characteristics of the lidar signals in the three cases and the corresponding wind velocities. "Lag" refers to the time elapsed following the launch of the rocket through lidar signal detection, and "Duration" refers to the time during which the plume signal continued to be detected by lidar.

The rocket plume was assumed to be carried by the wind, similarly to noctilucent clouds. Based on the observation that the thickness and altitude of the rocket plume remains relatively constant while it is detected by lidar, it is also assumed that the plume travels horizontally at a nearly constant altitude. As can be seen from Fig. 9, it then becomes possible to estimate the distance to the ejection point of the rocket plume and its spread. However, it must be noted that such estimations ignore horizontal diffusion speed and the initial velocity of the plume (the initial velocity of the plume is not known). The Estimations are presented in Table 3.

The results in Table 3 consist of extremely rough estimates, but it is particularly interesting that these estimates indicate that the plume seems to be spread out over a range wider than the horizontal distance between the rocket and the lidar observation site. This result is partly due to the error caused by ignoring initial velocity, but even if initial velocity were to be taken into consideration, the results still point to the potential application of this method to an interesting measurement experiment involving the diffusion of concentrated aerosols in the mesosphere. Further, if estimation of the particle-size distribution of the rocket plume material were possible to some degree, the particle density could be calculated using the lidar signal data, which in turn would allow the estimation of the vertical diffusion coefficient. If such measurements can be made with precision, the calculated diffu-
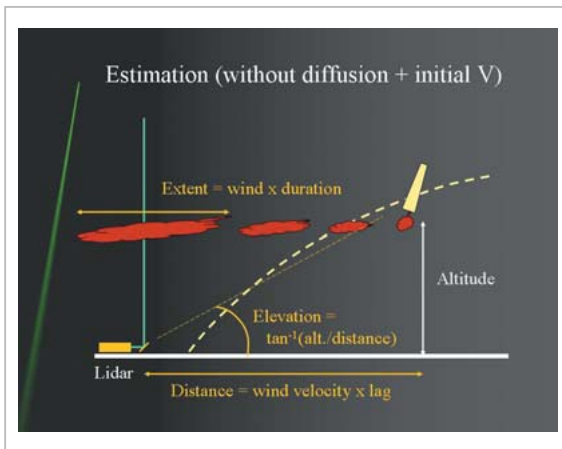
Fig.9 *Schematic diagram of rocket plume and lidar detection*

Table 2 *Characteristics of Rocket Plume Signals and Wind Velocities*

Date [AKST]	1999/01/21	1999/02/10	2000/02/24
Launch time	28:57	21:45	22:45
Lag	18 min	80 (or 45) min	30 min
Duration	30 min	54 (or 89) min	80 min
Altitude	～ 80 km	～ 68 km	～ 68 km
thickness	1 ～ 6 km	～ 4 km	～ 4 km
N‑S wind	～ 30 m/s S	～ 30 m/s S	～ 50-30 m/s S
E–W wind	～ 15 m/s E	～ 15 m/s E	～ 0 m/s

Table 3 *Information Obtained from the Rocket Plume Data*

Date [AKST]	21/01/1999	10/02/1999	24/02/2000
Horizontal distance	∼ 32 km	∼ 144 (81) km	∼ 90 km
Elevation angle	∼ 68°	∼ 25° (40°)	∼ 37°
Horizontal extent	∼ 54 km	∼ 97 (160) km	∼ 144 - 240 km

sion coefficients may be applied to data for noctilucent clouds, which are natural aerosols, and may open the way to a number of new studies.

We are grateful to the laboratory staff members of NICT, the University of Alaska, Fairbanks, and the Poker Flat Research Range, all of whom offered their support in the observations conducted in the course of this work.

References

1 B. Fogle and B. Haurwitz, "Noctilucent clouds", Space Science Reviews, 6, 1966.

2 G. E. Thomas, et al., "Relation Between increasing methane and the presence of ice clouds at the mesopause", Nature, 338, 490-492, 1989.

3 K. Mizutani et al., "Rayleigh and Rayleigh Doppler lidars for the observations of the Arctic middle atmosphere", IEICE trans. Commun., E83-B, 9, 2004-2009, 2000.

4 Y. Murayama et al., "Medium frequency radar in Japan and Alaska for upper atmosphere observations", IEICE trans. Commun., E83-B, 9, 1996-2003, 2000.

5 NICT Aurora Live, http://salmon.nict.go.jp/awc/contents/

6 U. von Zhan, et al., "Noctilucent clouds and the mesospheric water vapour: the past decade", Atmos. Chem. Phys,. 4, 2449-2464, 2004.

7 T. Sugiyama, et al., "Oscillation in polar mesospheric summer echoes and bifurcation of noctilucent cloud formation", Geophys. Res. Lett., 23(6), 653-656, 1996.

SAKANOI Kazuyo, *Dr. Sci.*

Komazawa University

Dynamics in the Thermosphere and Mesosphere

Richard L. COLLINS, *Ph.D.*

Associate Professor, University of Alaska Fairbanks

Aeronomy and Laser Remote Sensing

MURAYAMA Yasuhiro, *Dr. Eng.*

Planning Manager, Strategic Planning Office, Strategic Planning Department

Dynamics in the Thermosphere and Mesosphere

MIZUTANI Kohei, *Ph.D.*

Research Manager, Environment Sensing and Network Group, Applied Electromagnetic Research Center

Laser Remote Sensing